

Communication

Two-Dimensional Quantum Droplets in Binary Dipolar Bose-Bose Mixture

Aowei Yang ^{1,†}, Guilong Li ^{1,†} , Xunda Jiang ¹, Zhiwei Fan ², Zhaopin Chen ³, Bin Liu ^{1,*} and Yongyao Li ¹

¹ Guangdong-Hong Kong-Macao Joint Laboratory for Intelligent Micro-Nano Optoelectronic Technology, School of Physics and Optoelectronic Engineering, Foshan University, Foshan 528225, China

² Department of Physics, University of Bath, Bath BA2 7AY, UK

³ Physics Department and Solid-State Institute, Technion, Haifa 32000, Israel

* Correspondence: binliu@fosu.edu.cn

† These authors contributed equally to this work.

Abstract: We study two-dimensional (2D) isotropic quantum droplets (QDs) in dipolar binary Bose–Einstein condensates (BECs). The QDs are supported by the competition between the 2D form of the Lee–Huang–Yang (LHY) term and the isotropic dipole–dipole interactions (DDIs). Moreover, the DDIs in the 2D plane can be tuned to be either repulsive or attractive. Before that, QDs in dipolar BECs were often explored in three-dimensional (3D) systems, with competition between the attractive DDIs and the repulsive LHY term. Unlike the 3D system, the LHY term of the 2D binary system behaves in a logarithmic form, which can feature both attraction and repulsion. In this case, the QDs can be produced regardless of the interactions (attraction, repulsion, or zero) that the mean-field effect represents. In this paper, we model the aforementioned QDs via the 2D binary dipolar BECs with the competition between isotropic DDIs and the logarithmic LHY term. Their characteristic parameters (the peak density, I_p , chemical potential, μ , and effective area, A_{eff}) using both numerical and theoretical methods are discussed. The centripetal collision and oblique collision between moving QDs are also studied.

Keywords: quantum droplets; dipolar binary Bose–Einstein condensates; Lee–Huang–Yang term



Citation: Yang, A.; Li, G.; Jiang, X.; Fan, Z.; Chen, Z.; Liu, B.; Li, Y. Two-Dimensional Quantum Droplets in Binary Dipolar Bose–Bose Mixture. *Photonics* **2023**, *10*, 405. <https://doi.org/10.3390/photonics10040405>

Received: 10 February 2023

Revised: 23 March 2023

Accepted: 3 April 2023

Published: 4 April 2023



Copyright: © 2023 by the authors. Licensee MDPI, Basel, Switzerland. This article is an open access article distributed under the terms and conditions of the Creative Commons Attribution (CC BY) license (<https://creativecommons.org/licenses/by/4.0/>).

1. Introduction

According to mean-field (MF) theory, a condensed bosonic mixture collapses when the interspecies attraction becomes stronger than the geometrical average of the intraspecies repulsions [1,2], $g_{12}^2 > g_{11}g_{22}$. Perhaps the most effective solution to tackling the collapses has recently been theoretically presented [3] and experimentally implemented [4–16]. It is based on the LHY correction provided by quantum fluctuations to the MF dynamics of BECs [17–20]. In binary BECs, the interaction between atoms is nearly eliminated by modifying the repulsion within the component and the attraction between the components using the Feshbach resonance technique [21]. These soliton-like states, called Quantum droplets, are formed as a result of the equilibrium between the MF dynamics and beyond the mean-field (BMF) effect, which is effectively represented by the famous LHY term, i.e., the local quartic self-repulsive term in the 3D Gross–Pitaevskii equations (GPEs).

Subsequently, the theoretical scheme was extended from 3D systems to low-dimensional systems, and the specific expressions for the LHY terms in two- and one-dimensional systems were re-derived and modified [22]. However, in the two-dimensional (2D) case, the LHY term is very intriguing because it is proportional to $n[\ln(n/n_0) - 1]$ (n_0 is the equilibrium density). Due to the nature of the logarithmic function, this LHY correction can show both attraction and repulsion. This characteristic indicates that whether the MF interaction is attractive or repulsive, it could be used to create a QD with LHY corrections in 2D binary BECs.

The MF attraction can be provided not only by cubic contact (local) inter-component attraction in binary BEC [23–46], but also by long-range (nonlocal) dipole–dipole inter-

actions in a single-component condensate of atoms carrying permanent magnetic moments [12,47–50]. The situation of a single-component dipolar BECs system has drawn much attention [51–54]. However, in this system framework, the conflict between the higher-order repulsive LHY term and attractive DDIs has been mentioned frequently. Regarding the scenario involving DDIs in a low-dimensional two-component system, some relevant reports consider this proposal [55–58]. When we discuss low-dimensional binary dipolar BECs, especially in the 2D case, unlike the initial stereotypical repulsive effect, the logarithmic LHY term at a 2D dynamic will expand the system’s options.

It is worth noting that in prior 2D dipolar BECs studies, the polarization direction of the dipoles is required to be parallel to the 2D plane to ensure the generally attractive DDIs, which can form QDs in equilibrium with the repulsive LHY term [59,60]. If the dipole is perpendicular to the 2D plane, QDs cannot be formed unless the rotation field effect is introduced to tune the effective dipole coupling from the positive value to negative value through the rapid rotation of the dipole direction [61–63]. Whether repulsive DDIs and beyond mean-field effects can form QDs in a 2D dipolar BECs system is still debatable. Yet, this problem has an entirely new possible solution since the LHY term in the 2D binary system is in logarithmic form.

We consider DDIs in 2D binary Bose-Bose mixtures with all the dipoles oriented perpendicular to the 2D plane and theoretically construct the QDs supported by the combination of the logarithmic LHY correction and MF interaction. In the current formula, not only attractive DDIs, but also repulsive DDIs can form QDs because the LHY correction can be adaptively changed into attraction or repulsion. We also discuss how QDs behave in this physical environment and how their collision dynamics perform.

The rest of the paper is structured as follows. The model is introduced in Section 2. Basic numerical and theoretical results of QDs are presented in Section 3. Then, the collisions between the moving QDs are reported in Section 4. The work is concluded in Section 5.

2. Model

We consider isotropic QDs in Petrov’s proposal [22] trapped in a 2D binary dipolar BEC system with all the dipoles oriented perpendicular to the 2D plane (as shown in Figure 1). The GPE-LHY of this system is

$$i\frac{\partial\psi_+}{\partial t} = -\frac{1}{2}\nabla^2\psi_+ + \kappa\psi_+(\mathbf{r}) \iint d\mathbf{r}'R(\mathbf{r}-\mathbf{r}')\left[|\psi_+(\mathbf{r}')|^2 + |\psi_-(\mathbf{r}')|^2\right] + \gamma\psi_+\left[|\psi_+(\mathbf{r}')|^2 + |\psi_-(\mathbf{r}')|^2\right] \ln\left[|\psi_+(\mathbf{r}')|^2 + |\psi_-(\mathbf{r}')|^2\right], \tag{1}$$

$$i\frac{\partial\psi_-}{\partial t} = -\frac{1}{2}\nabla^2\psi_- + \kappa\psi_-(\mathbf{r}) \iint d\mathbf{r}'R(\mathbf{r}-\mathbf{r}')\left[|\psi_-(\mathbf{r}')|^2 + |\psi_+(\mathbf{r}')|^2\right] + \gamma\psi_-\left[|\psi_-(\mathbf{r}')|^2 + |\psi_+(\mathbf{r}')|^2\right] \ln\left[|\psi_-(\mathbf{r}')|^2 + |\psi_+(\mathbf{r}')|^2\right]. \tag{2}$$

If we consider a symmetry form (here, we assumed that $\psi_+ = \psi_- = \psi/\sqrt{2}$), the GPE-LHY can be expressed as

$$i\frac{\partial}{\partial t}\psi = -\frac{1}{2}\nabla^2\psi + \kappa\psi \int R(\mathbf{r}-\mathbf{r}')|\psi(\mathbf{r}')|^2d\mathbf{r}' + \gamma|\psi|^2\psi \ln|\psi|^2, \tag{3}$$

where $\mathbf{r} = (x,y)$ is the set of the coordinates, ψ is the wave function, and κ is the strength of the DDI. Notably, κ is an adjustable quantity, i.e., its sign can be positive or negative, and the total nonlocal interaction can be adjusted to become repulsive or attractive. γ is the coefficient of the beyond-MF effect in 2D binary BECs. The isotropic kernel corresponding to the particles’ dipolar moments polarized perpendicular to the (x,y) plane is defined as

$$R(\mathbf{r}-\mathbf{r}') = \frac{1-3\cos^2\Theta}{[b^2+(\mathbf{r}-\mathbf{r}')^2]^{3/2}}, \tag{4}$$

where b is the cutoff of the kernel, which is determined by the confinement length a_{\perp} in the transverse dimension [64–66]. In our isotropic 2D system, the angle Θ between the dipole polarization direction and its relative distance is $\frac{\pi}{2}$, i.e., $\cos^2 \Theta = 0$. Furthermore, if we apply a notation

$$t \leftarrow \gamma t, (x, y) \leftarrow \sqrt{\gamma}(x, y), \kappa \leftarrow \frac{\kappa}{\gamma}, \tag{5}$$

Equation (3) can be simplified as

$$i \frac{\partial}{\partial t} \psi = -\frac{1}{2} \nabla^2 \psi + \kappa \psi \int R(\mathbf{r} - \mathbf{r}') |\psi(\mathbf{r}')|^2 d\mathbf{r}' + |\psi|^2 \psi \ln |\psi|^2, \tag{6}$$

the total energy of the system is

$$E = \frac{1}{2} \int d\mathbf{r} \left[|\nabla \psi|^2 + \kappa |\psi|^2 \int R(\mathbf{r} - \mathbf{r}') |\psi(\mathbf{r}')|^2 d\mathbf{r}' + |\psi|^4 \ln \left(\frac{|\psi|^2}{\sqrt{e}} \right) \right], \tag{7}$$

and the total number of particles is defined as

$$N = \int |\psi|^2 d\mathbf{r}. \tag{8}$$

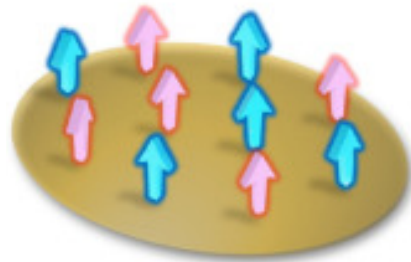


Figure 1. Schematic diagram of the 2D binary dipolar system plane, with all the dipoles oriented perpendicular to the 2D plane. The two types of arrows with different colors (pink and blue) represent the two components of dipolar atoms in the mixture.

While units are not required in the figures shown below, because all the quantities in Equations (6)–(8) are written in scaled form, it is relevant to summarise here estimates for the pertinent quantities in physical units. To achieve this, we need to convert the results into physical units that correspond to the experimental realization of QDs in Bose-Bose mixtures, using the values of the magnetic moment for ^{164}Dy atoms. The typical size of confinement length in underlying physical units is $a_{\perp} \sim 3 \mu\text{m}$ [67–70]. We thus conclude that the stable 2D binary dipolar QDs may be created with the number of atoms in the range from $N_{atom} \sim 10^3$ to $N_{atom} \sim 10^4$, and physical lateral sizes $l_{phys} \sim 1 \mu\text{m}$. The corresponding relation between the physical quantities and scaled ones is

$$N_{atom} \sim 10 N, (x, y)_{phys} \sim (x, y) \times 1 \mu\text{m}. \tag{9}$$

The stationary solution is obtained as a usual form with the wavefunction $\phi(\mathbf{r})$ and real chemical potential μ , i.e.,

$$\psi(\mathbf{r}, t) = \phi(\mathbf{r}) e^{-i\mu t}. \tag{10}$$

A dynamical invariant of the system is the total norm, which is proportional to the total number of atoms in the dipolar bosonic mixtures. The free control parameters in the system are the strength of the DDI, κ , and the total norm of the QDs, N .

3. Stationary Solution of the Quantum Droplets

The isotropic QDs in this system are numerically found using the imaginary-time method (ITM) [71,72] by inputting a special ansatz

$$\phi^{(0)}(x, y) = A\tilde{r} \exp(-\alpha\tilde{r}^2). \tag{11}$$

where $A > 0$ and $\alpha > 0$ are real constants. $\tilde{r} = \sqrt{x^2 + y^2}$.

Typical examples of stable fundamental QDs are shown in Figure 2a,b. The size of the QDs created by the attractive DDI with $\kappa = -0.05$ is smaller than another with $\kappa = 0.05$. The stability of the fundamental QDs is demonstrated by direct simulation with 1% random noise, as plotted in Figure 2c,d. This result demonstrates that both attracting and repelling DDIs can create stable self-localized states in 2D dipolar binary BECs. At the equilibrium condition, the QD is a flat-top QD; hence, we can neglect the contribution from the kinetic energy term by applying the Thomas–Fermi (TF) approximation. In this case, the density distribution of the QDs satisfies $n(\mathbf{r}) = |\psi(\mathbf{r})|^2 = \text{const}$. Therefore, the total energy (7) is

$$E = \frac{1}{2} \left(\kappa \varepsilon n^2 + n^2 \ln\left(\frac{n}{\sqrt{e}}\right) \right) A_S, \tag{12}$$

where $A_S = N/n$ is the total area of the QDs and $\varepsilon = \int d\mathbf{r} R(\mathbf{r}) \approx 6.2$ is the totally nonlocal effect. Then, we can obtain the density value of the QD by solving $dE/dn = 0$, which yields the

$$n_e = \frac{1}{e^{1/2} e^{\kappa \varepsilon}}, \tag{13}$$

and the chemical potential is

$$\mu_e = \kappa \varepsilon n_e + n_e \ln n_e. \tag{14}$$

If we replace $n_e = N/A_S$, substitute it into Equation (12), and then solve $dE/dA_S = 0$, one can obtain the total area for the equilibrium state satisfying the equation

$$\ln A_S = \kappa \varepsilon + \ln N + \frac{1}{2}. \tag{15}$$

To study the characteristics of the QDs, we define the effective area for the QDs as

$$A_{\text{eff}} = \frac{(\int |\phi|^2 d\mathbf{r})^2}{\int |\phi|^4 d\mathbf{r}}. \tag{16}$$

The peak density (I_P), chemical potential (μ), and effective area (A_{eff}) of the fundamental QDs as functions of N for repulsive and attractive DDIs are displayed in Figure 3(a1–b3), respectively. When the MF interaction and LHY term compete, a superfluid, incompressible state is maintained, whose density (at extremely low values) cannot rise above a particular maximum. Thus, this quantum macroscopic state is referred to as a fluid, and localized states filled by it are referred to as “droplets” [4]. In Figure 3(a1,b1), the peak values saturate at $I_P \approx 0.472$ and $I_P \approx 0.837$, respectively, if N is sufficiently large, as may be expected for the QDs. According to Equation (13), their theoretical prediction equilibrium densities are $n_e \approx 0.445$ and $n_e \approx 0.827$, which are also close to the numerical results [see the red dashed line in Figure 3(a1,b1)].

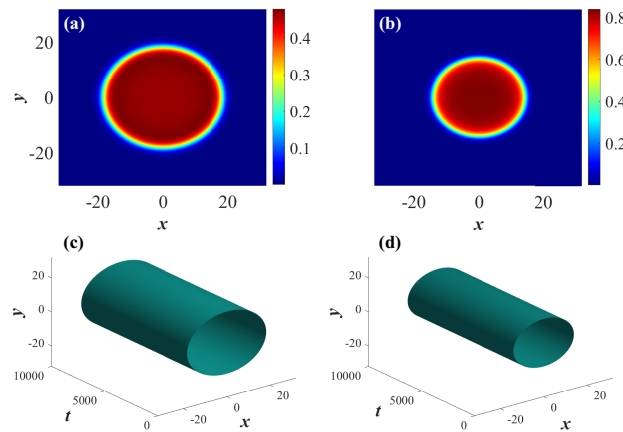


Figure 2. Typical examples of the stable fundamental QDs produced by Equation (4). Panels (a,b) display the density profiles of the QDs with $(N, \kappa) = (1000, 0.05)$ and $(1000, -0.05)$. (c,d) The perturbed evolutions of the QDs shown in Panels (a,b), produced by simulations of Equation (4) with 1% random noise added to the input.

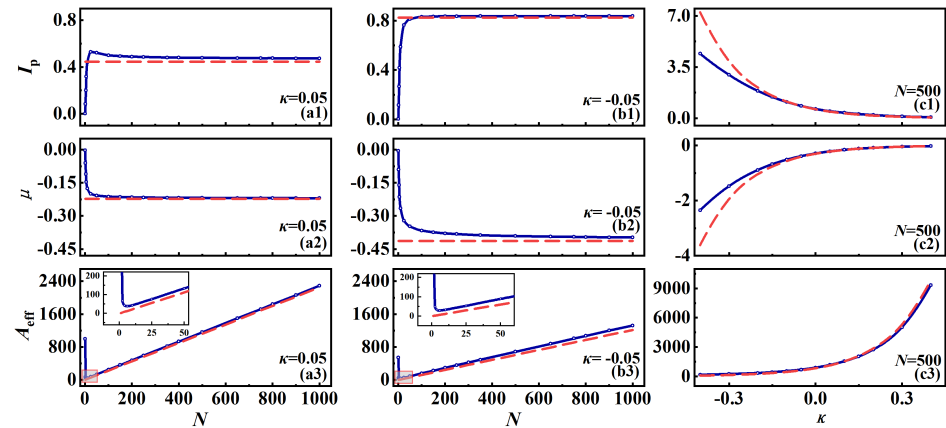


Figure 3. The first column (a1–a3): the peak density (I_p), chemical potential (μ), effective area (A_{eff}) of the fundamental QDs as functions of N for repulsive DDIs with $\kappa = 0.05$. The second column (b1–b3): the I_p , μ , and A_{eff} of the fundamental QDs as functions of N for attractive DDIs with $\kappa = -0.05$. The last column (c1–c3): the I_p , μ , and A_{eff} of the fundamental QDs as functions of the strength of κ with $N = 500$. Here, the blue curves are the results of the numerical calculation, and the red dashed curves in the panels are calculated from Equations (13), (14), and (15), respectively.

Figure 3(a2,b2) shows that the chemical potential decreases with an increasing N , i.e., $\frac{d\mu}{dN} < 0$, which indicates that it satisfies the Vakhitov–Kolokolov (VK) criterion, which is the well-known necessary stability condition for self-trapped modes [73]. This criterion has a straightforward physical interpretation: If we introduce one particle into the system and the energy of this bound state falls, the system is stable. They saturate at $\mu \approx -0.219$ and $\mu \approx -0.397$ when N is sufficiently large. The theoretical predictions of the chemical potential are $\mu_e \approx -0.222$ and $\mu_e \approx -0.414$, which are also close to the numerical results [see the red dashed line in Figure 3(a2,b2)].

When κ is positive, the dipole interaction shows repulsion, and in this case, I_p significantly increase with an increasing N at the beginning [at approximately $N < 25$], then I_p gradually decreases with an increasing N until it reaches equilibrium. The changing trend of the effective area in Figure 3(a3) reveals the cause of this phenomenon. In this case, QDs were not formed as expected because when N is very small (just a few particles), its size is enormous and comparable to the gas state. At this point, the system will be encouraged by the increase in the number of atoms to produce droplets of condensate, which causes the effective area A_{eff} to decrease rapidly and the corresponding peak density I_p to increase

rapidly. The peak density of the QD remains static once it enters equilibrium due to its incompressibility; hence, the effective area A_{eff} grows linearly as N increases.

When κ is negative, the dipole interaction exhibits attraction, and the situation is similar to that mentioned above. The peak density of the negative κ increases continuously, while the other peak density increases first and then falls because the effective area of the latter increases more quickly than the former.

The I_p , μ , and A_{eff} of the fundamental QDs as functions of the strength of κ with $N = 500$ are also shown in Figure 3(c1–c3). The numerical results are consistent with those of the theoretical analysis.

4. Collision between the Moving Quantum Droplets

Stable 2D dipolar binary BEC mixtures can be set in motion by opposite kicks $\pm\eta$ applied along the x or y -direction. Accordingly, it is possible to simulate collisions between two mixtures moving in opposite directions. Collisions in the x and y directions behave similarly due to the isotropic properties. Without loss of generality, we discuss centripetal collisions that occur in the x direction. Generally, the initial states for both moving QDs can be constructed as follows:

$$\phi(x, y) = \phi(x - x_0, y)e^{-i\eta x} + \phi(x + x_0, y)e^{i\eta x}. \tag{17}$$

Several typical collision results are shown in Figure 4. We investigate the binary collisions between QDs created in 2D dipolar binary BECs and distinguish between the separation and merging as the two main outcomes, i.e., quasi-elastic collisions and completely inelastic collisions. The quasi-elastic collisions will merge at the beginning, but when compressed to the limit, they will split along the positive and negative directions of the y axis; that is, they will deflect with an angle of 90 degrees relative to the motion before the collision, as shown in Figure 4(a1–a6). Similar results have been reported in Ref. [74]. The completely inelastic collisions are displayed in Figure 4(b1–b6). Two QDs merge into a quadrupolar breather, repeatedly elongating and oscillating along the y and x directions.

In the present setting, the simulations show that the values of κ will affect the results of collisions. When $\kappa > 0$, for instance, quasi-elastic collision is more likely to occur than when $\kappa < 0$. This might result from the repulsive interaction of DDIs, which produces a low surface tension that cannot absorb the collision pair’s kinetic energy [75].

Depending on the pair’s collision velocity, which is proportional to η , the increase in η leads to a transition from completely inelastic collisions between slow QDs to quasi-elastic outcomes for fast QDs. When η becomes too large, the collision will split the initial binary mixture into several pieces, as shown in Figure 4(c1–c6). In addition, the values of N mainly affect the size of droplets, which will cause the critical velocity that discriminates between the completely inelastic and quasi-elastic cases to display a different dependence on the norm N for small and large droplets [8].

We also discuss the collision dynamics between two QDs whose centers of mass are not at the same level, i.e., off-center collisions. In our simulations, we move the two mixtures by a distance of y_0 in the positive and negative directions of the y axis and then apply appropriate opposite kicks $\pm\eta$. The initial states for these moving QDs can be constructed as follows:

$$\phi(x, y) = \phi(x - x_0, y - y_0)e^{-i\eta x} + \phi(x + x_0, y + y_0)e^{i\eta x}, \tag{18}$$

and a typical result is shown in Figure 4(d1–d6). We find that the formation of a rotating quadrupolar breathing body is the result of an oblique collision. Some characteristics of the collision result, such as the rotational speed and the duration of the breathing motion, are affected by the values of κ , N , y_0 , and η . Of course, an excessive η will also cause the mixture to separate.

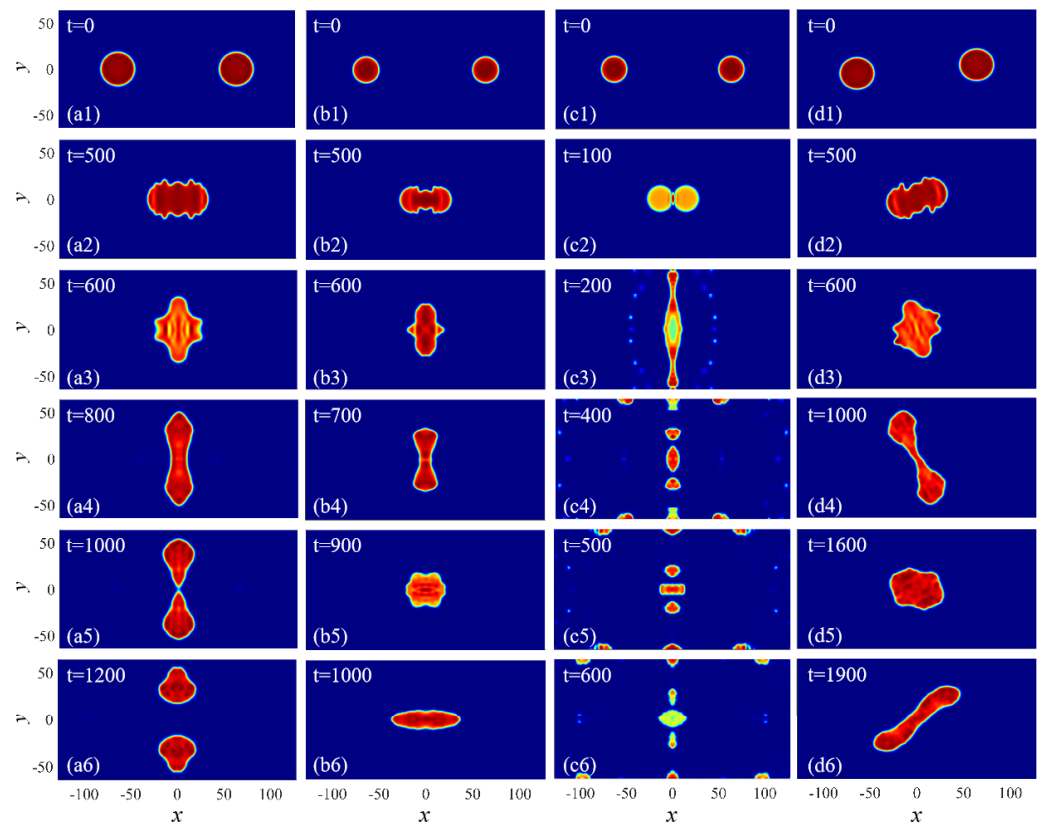


Figure 4. Several typical examples of colliding QDs. (a–c) The collision of two QDs by inputting Equation (17) with $x_0 = 64$ and the norm of each QD $N = 500$. (a1–a6) Quasi-elastic collisions between two QDs with $\kappa = 0.05$ and $\eta = 0.1$. (b1–b6) Completely inelastic collisions between two QDs with $\kappa = -0.05$ and $\eta = 0.1$. (c1–c6) Collisions between two QDs with $\kappa = -0.05$ and $\eta = 0.5$. (d1–d6) The off-center collision of two QDs by input Equation (18) with $x_0 = 64$ and $y_0 = 10$; the other parameters are $\kappa = 0.05$ and $\eta = 0.1$.

5. Conclusions

Based on the adaptive balance mechanism of the LHY term in the 2D binary BECs that represents the correction of the beyond mean-field effects, we prove that both repulsive and attractive DDIs can construct 2D isotropic QDs in a binary dipolar BEC system with all the dipoles oriented perpendicular to the 2D plane. We discuss the characteristic parameters of the QDs formed by the combination of attracting or repelling DDIs and the logarithmic LHY term, and the numerical results are consistent with the theoretical predictions. In addition, we also discussed the collision dynamics under this physical setting from the two cases of centripetal collision and non-centripetal collision. The numerical simulation results show that when the collision velocity is appropriate, there will be completely inelastic collisions and quasi-elastic collisions, while a large collision velocity will destroy the mixtures and split them into multiple components.

The present analysis can be extended further. First, the QDs outlined above are fundamental modes, and it is natural to expect that the vortex (alias spinning) modes may offer an opportunity to study more sophisticated properties of the QD state of matter. Furthermore, anisotropic QD embedded vorticity has been constructed in a 2D binary dipolar system [60]. Another relevant possibility is constructing anisotropic QD modes with vorticity in a 3D binary dipolar BEC system, which will be intriguing and challenging.

Author Contributions: Conceptualization, X.J., Z.F., Z.C., B.L. and Y.L.; Software, A.Y. and G.L. All authors have read and agreed to the published version of the manuscript.

Funding: This research was funded by Natural Science Foundation of Guangdong province (2021A1515010214), NNSFC (China) (12274077,11905032, 11874112, 11904051), Guang Dong Basic and Applied Basic Research Foundation (2021A1515111015); Key Research Projects of General Colleges in Guangdong Province (2019KZDXM001), Special Funds for the Cultivation of Guangdong College Students Scientific and Technological Innovation (pdjh2021b0529, pdjh2022a0538), Research Fund of Guangdong-Hong Kong-Macao Joint Laboratory for Intelligent Micro-Nano Optoelectronic Technology (2020B1212030010).

Data Availability Statement: Not applicable.

Conflicts of Interest: The funders had no role in the design of the study; in the collection, analyses, or interpretation of data; in the writing of the manuscript, or in the decision to publish the results.

References

1. Donley, E.A.; Claussen, N.R.; Cornish, S.L.; Roberts, J.L.; Cornell, E.A.; Wieman, C.E. Dynamics of collapsing and exploding Bose–Einstein condensates. *Nature* **2001**, *412*, 295–299. [[CrossRef](#)] [[PubMed](#)]
2. Malomed, B.A. Multidimensional Solitons: Well-Established Results and Novel Findings. *Eur. Phys. J. Spec. Top.* **2016**, *225*, 2507–2532. [[CrossRef](#)]
3. Petrov, D.S. Quantum Mechanical Stabilization of a Collapsing Bose-Bose Mixture. *Phys. Rev. Lett.* **2015**, *115*, 155302. [[CrossRef](#)] [[PubMed](#)]
4. Cabrera, C.R.; Tanzi, L.; Sanz, J.; Naylor, B.; Thomas, P.; Cheiney, P.; Tarruell, L. Quantum liquid droplets in a mixture of Bose–Einstein condensates. *Science* **2018**, *359*, 301–304. [[CrossRef](#)]
5. Semeghini, G.; Ferioli, G.; Masi, L.; Mazzinghi, C.; Wolswijk, L.; Minardi, F.; Modugno, M.; Modugno, G.; Inguscio, M.; Fattori, M. Self-Bound Quantum Droplets of Atomic Mixtures in Free Space. *Phys. Rev. Lett.* **2018**, *120*, 235301. [[CrossRef](#)]
6. Chomaz, L.; Baier, S.; Petter, D.; Mark, M.J.; Wächtler, F.; Santos, L.; Ferlaino, F. Quantum-Fluctuation-Driven Crossover from a Dilute Bose–Einstein Condensate to a Macrodroplet in a Dipolar Quantum Fluid. *Phys. Rev. X* **2016**, *6*, 041039. [[CrossRef](#)]
7. Cheiney, P.; Cabrera, C.R.; Sanz, J.; Naylor, B.; Tanzi, L.; Tarruell, L. Bright soliton to quantum droplet transition in a mixture of Bose–Einstein condensates. *Phys. Rev. Lett.* **2018**, *120*, 135301. [[CrossRef](#)]
8. Ferioli, G.; Giulia, S.; Masi, L.; Giusti, G.; Modugno, G.; Inguscio, M. Gallemí, A.; Recati, A.; Fattori, M. Collisions of Self-Bound Quantum Droplets. *Phys. Rev. Lett.* **2019**, *122*, 090401. [[CrossRef](#)]
9. D’Errico, C.; Burchianti, A.; Prevedelli, M.; Salasnich, L.; Ancilotto, F.; Modugno, M.; Fort, C. Observation of quantum droplets in a heteronuclear bosonic mixture. *Phys. Rev. Res.* **2019**, *1*, 033155. [[CrossRef](#)]
10. Ferrier-Barbut, I.; Kadau, H.; Schmitt, M.; Wenzel, M.; Pfau, T. Observation of Quantum Droplets in a Strongly Dipolar Bose Gas. *Phys. Rev. Lett.* **2016**, *116*, 215301. [[CrossRef](#)]
11. Ferrier-Barbut, I.; Wenzel, M.; Schmitt, M.; Böttcher, F.; Pfau, T. Onset of a modulational instability in trapped dipolar Bose–Einstein condensates. *Phys. Rev. A* **2018**, *97*, 011604. [[CrossRef](#)]
12. Ferrier-Barbut, I.; Wenzel, M.; Böttcher, F.; Langen, T.; Isoard, M.; Stringari, S.; Pfau, T. Scissors Mode of Dipolar Quantum Droplets of Dysprosium Atoms. *Phys. Rev. Lett.* **2018**, *120*, 160402. [[CrossRef](#)] [[PubMed](#)]
13. Böttcher, F.; Wenzel, M.; Schmidt, J.N.; Guo, M.; Langen, T.; Ferrier-Barbut, I.; Mazzanti, F. Dilute dipolar quantum droplets beyond the extended Gross–Pitaevskii equation. *Phys. Rev. Res.* **2019**, *1*, 033088. [[CrossRef](#)]
14. Schmitt, M.; Wenzel, M.; Böttcher, F.; Ferrier-Barbut, I.; Pfau, T. Self-Bound Droplets of a Dilute Magnetic Quantum Liquid. *Nature* **2016**, *539*, 259–262. [[CrossRef](#)]
15. Ferrier-Barbut, I.; Schmitt, M.; Wenzel, M.; Kadau, H.; Pfau, T. Liquid quantum droplets of ultracold magnetic atoms. *J. Phys. B At. Mol. Opt. Phys.* **2016**, *49*, 214004. [[CrossRef](#)]
16. Kadau, H.; Schmitt, M.; Wenzel, M.; Wink, C.; Maier, T.; Ferrier-Barbut, I.; Pfau, T. Observing the Rosensweig Instability of a Quantum Ferrofluid. *Nature* **2016**, *530*, 194–197. [[CrossRef](#)]
17. Malomed, B.A. The Family of Quantum Droplets Keeps Expanding. *Front. Phys.* **2021**, *16*, 22504. [[CrossRef](#)]
18. Guo, M.Y.; Pfau, T. A New State of Matter of Quantum Droplets. *Front. Phys.* **2021**, *16*, 32202. [[CrossRef](#)]
19. Otajonov, S.R.; Otajonov, E.N.; Abdullaev, F.K. Modulational instability and quantum droplets in a two-dimensional Bose–Einstein condensate. *Phys. Rev. A* **2022**, *106*, 033309. [[CrossRef](#)]
20. Böttcher, F.; Schmidt, J.N.; Hertkorn, J.; Ng, K.S.H.; Graham, S.D.; Guo, M.Y.; Langen, T.; Pfau, T. New States of Matter with Fine-Tuned Interactions: Quantum Droplets and Dipolar Supersolids. *Rep. Prog. Phys.* **2021**, *84*, 012403. [[CrossRef](#)]
21. d’Errico, C.; Zaccanti, M.; Fattori, M.; Roati, G.; Inguscio, M.; Modugno, G.; Simoni, A. Feshbach resonances in ultracold ^{39}K . *New J. Phys.* **2007**, *9*, 223. [[CrossRef](#)]
22. Petrov, D.S.; Astrakharchik, G.E. Ultradilute Low-Dimensional Liquids. *Phys. Rev. Lett.* **2016**, *117*, 100401. [[CrossRef](#)]
23. Zheng, Y.Y.; Chen, S.T.; Huang, Z.P.; Dai, S.X.; Liu, B.; Li, Y.Y.; Wang, S.R. Quantum Droplets in Two-Dimensional Optical Lattices. *Front. Phys.* **2021**, *16*, 22501. [[CrossRef](#)]
24. Kartashov, Y.V.; Malomed, B.A.; Torner, L. Structured heterosymmetric quantum droplets. *Phys. Rev. Res.* **2020**, *2*, 033522. [[CrossRef](#)]

25. Otajonov, S.R.; Tsoy, E.N.; Abdullaev, F.K. Variational approximation for two-dimensional quantum droplets. *Phys. Rev. E* **2020**, *102*, 062217. [[CrossRef](#)]
26. Boudjemâa, A. Fluctuations and quantum self-bound droplets in a dipolar Bose-Bose mixture. *Phys. Rev. A* **2018**, *98*, 033612. [[CrossRef](#)]
27. Dong, L.; Qi, W.; Peng, P.; Wang, L.; Zhou, H.; Huang, C. Multi-stable quantum droplets in optical lattice. *Nonlinear Dyn.* **2020**, *102*, 303. [[CrossRef](#)]
28. Morera, I.; Astrakharchik, G.E.; Polls, A.; Juliá-Díaz, B. Quantum droplets of bosonic mixtures in a one-dimensional optical lattice. *Phys. Rev. Res.* **2020**, *2*, 022008. [[CrossRef](#)]
29. Liu, B.; Zhang, H.; Zhong, R.; Zhang, X.; Qin, X.; Huang, C.; Li, Y.; Malomed, B.A. Symmetry breaking of quantum droplets in a dual-core trap. *Phys. Rev. A* **2019**, *99*, 053602. [[CrossRef](#)]
30. Chen, Y.; Cai, X.; Liu, B.; Jiang, X.; Li, Y. Hidden vortices of quantum droplets in quasi-two dimensional space. *Acta Phys. Sin.* **2022**, *71*, 200302. [[CrossRef](#)]
31. Liu, B.; Chen, Y.; Yang, A.W.; Cai, X.Y.; Liu, Y.; Luo, Z.H.; Qin, X.Z.; Jiang, X.D.; Li, Y.Y.; Malomed, B.A. Vortex-ring quantum droplets in a radially-periodic potential. *New J. Phys.* **2022**, *24*, 123026. [[CrossRef](#)]
32. Dong, L.; Kartashov, Y.V. Rotating Multidimensional Quantum Droplets. *Phys. Rev. Lett.* **2021**, *126*, 244101. [[CrossRef](#)]
33. Huang, H.; Wang, H.; Chen, M.; Lim, C.; Wong, K. Binary-vortex quantum droplets. *Chaos Solitons Fractals* **2022**, *158*, 112079. [[CrossRef](#)]
34. Zhou, Z.; Shi, Y.; Ye, F.; Chen, H.; Tang, S.; Deng, H.; Zhong, H. Self-bound states induced by the Lee-Huang-Yang effect in non- \mathcal{PT} -symmetric complex potentials. *Nonlinear Dyn.* **2022**, *110*, 3769. [[CrossRef](#)]
35. Zhou, Z.; Shi, Y.; Tang, S.; Deng, H.; Wang, H.; He, X.; Zhong, H. Controllable dissipative quantum droplets in one-dimensional optical lattices. *Chaos Solitons Fractals* **2021**, *150*, 111193. [[CrossRef](#)]
36. Dong, L.W.; Liu, D.S.; Du, Z.J.; Shi, K.; Qi, W. Bistable multipole quantum droplets in binary Bose–Einstein condensates. *Phys. Rev. A* **2022**, *105*, 033321. [[CrossRef](#)]
37. Dong, L.W.; Shi, K.; Huang, C.M. Internal modes of two-dimensional quantum droplets. *Phys. Rev. A* **2022**, *106*, 053303. [[CrossRef](#)]
38. Xu, S.; Lei, Y.; Du, J.; Zhao, Y.; Hua, R.; Zeng, J. Three-dimensional quantum droplets in spin–orbit-coupled Bose–Einstein condensates. *Chaos Solitons Fractals* **2022**, *164*, 112665. [[CrossRef](#)]
39. Li, Y.Y.; Luo, Z.H.; Liu, Y.; Chen, Z.P.; Huang, C.Q.; Fu, S.H.; Tan, H.S.; Malomed, B.A. Two-dimensional solitons and quantum droplets supported by competing self- and cross-interactions in spin–orbit-coupled condensates. *New J. Phys.* **2017**, *19*, 113043. [[CrossRef](#)]
40. Cui, X. Spin-orbit-coupling-induced quantum droplet in ultracold Bose–Fermi mixtures. *Phys. Rev. A* **2018**, *98*, 023630. [[CrossRef](#)]
41. Wang, Y.; Guo, L.; Yi, S.; Shi, T. Theory for self-bound states of dipolar Bose–Einstein condensates. *Phys. Rev. Res.* **2020**, *2*, 043074. [[CrossRef](#)]
42. Wang, J.; Hu, H.; Liu, X.J. Thermal destabilization of self-bound ultradilute quantum droplets. *New J. Phys.* **2020**, *22*, 103044. [[CrossRef](#)]
43. Guo, Z.; Jia, F.; Li, L.; Ma, Y.; Hutson, J.; Cui, X.; Wang, D. Lee-Huang-Yang effects in the ultracold mixture of ^{23}Na and ^{87}Rb with attractive interspecies interactions. *Phys. Rev. Res.* **2021**, *3*, 033247. [[CrossRef](#)]
44. Guebli, N.; Boudjemâa, A. Quantum self-bound droplets in Bose-Bose mixtures: Effects of higher-order quantum and thermal fluctuations. *Phys. Rev. A* **2021**, *104*, 023310. [[CrossRef](#)]
45. Boudjemâa, A. Many-body and temperature effects in two-dimensional quantum droplets in Bose-Bose mixtures. *Sci. Rep.* **2021**, *11*, 21765. [[CrossRef](#)]
46. Jiang, X.; Zeng, Y.; Ji, Y.; Liu, B.; Qin, X.; Li, Y. Vortex formation and quench dynamics of rotating quantum droplets. *Chaos Solitons Fractals* **2022**, *161*, 112368. [[CrossRef](#)]
47. Wächtler, F.; Santos, L. Quantum filaments in dipolar Bose–Einstein condensates. *Phys. Rev. A* **2016**, *93*, 061603(R). [[CrossRef](#)]
48. Wächtler, F.; Santos, L. Ground-state properties and elementary excitations of quantum droplets in dipolar Bose–Einstein condensates. *Phys. Rev. A* **2016**, *94*, 043618. [[CrossRef](#)]
49. Sekino, Y.; Nishida, Y. Quantum droplet of one-dimensional bosons with a three-body attraction. *Phys. Rev. A* **2018**, *97*, 011602(R). [[CrossRef](#)]
50. Bisset, R.N.; Wilson, R.M.; Baillie, D.; Blakie, P.B. Ground-state phase diagram of a dipolar condensate with quantum fluctuations. *Phys. Rev. A* **2016**, *94*, 033619. [[CrossRef](#)]
51. Cidrim, A.; dos Santos, F.E.A.; Henn, E.A.L.; Macrì, T. Vortices in self-bound dipolar droplets. *Phys. Rev. A* **2018**, *98*, 023618. [[CrossRef](#)]
52. Baillie, D.; Wilson, R.M.; Bisset, R.N.; Blakie, P.B. Self-bound dipolar droplet: A localized matter wave in free space. *Phys. Rev. A* **2016**, *94*, 021602(R). [[CrossRef](#)]
53. Boudjemâa, A. Two-Dimensional Quantum Droplets in Dipolar Bose Gases. *New J. Phys.* **2019**, *21*, 093027. [[CrossRef](#)]
54. Edler, D.; Mishra, C.; Wächtler, F.; Nath, R.; Sinha, S.; Santos, L. Quantum Fluctuations in Quasi-One-Dimensional Dipolar Bose–Einstein Condensates. *Phys. Rev. Lett.* **2017**, *119*, 050403. [[CrossRef](#)]
55. Bland, T.; Poli, E.; Ardila, L.A.P.; Santos, L.; Ferlaino, F.; Bisset, R.N. Alternating-domain supersolids in binary dipolar condensates. *Phys. Rev. A* **2022**, *106*, 053322. [[CrossRef](#)]

56. Bisset, R.N.; Ardila, L.A.P.; Santos, L. Quantum Droplets of Dipolar Mixtures. *Phys. Rev. Lett.* **2021**, *126*, 025301. [[CrossRef](#)] [[PubMed](#)]
57. Smith, J.C.; Baillie, D.; Blakie, P.B. Quantum Droplet States of a Binary Magnetic Gas. *Phys. Rev. Lett.* **2021**, *126*, 025302. [[CrossRef](#)]
58. Scheiermann, D.; Ardila, L.A.P.; Bland, T.; Bisset, R.N.; Santos, L. Catalyzation of supersolidity in binary dipolar condensates. *arXiv* **2022**, arXiv:2202.08259.
59. Tikhonenkov, I.; Malomed, B.A.; Vardi, A. Anisotropic solitons in dipolar Bose–Einstein Condensates. *Phys. Rev. Lett.* **2008**, *100*, 090406. [[CrossRef](#)] [[PubMed](#)]
60. Li, G.L.; Jiang, X.D.; Liu, B.; Chen, Z.P.; Malomed, B.A.; Li, Y.Y. Anisotropic vortex quantum droplets in dipolar Bose–Einstein condensates. *arXiv* **2023**, arXiv:2301.04305.
61. Giovanazzi, S.; Görlitz, A.; Pfau, T. Tuning the Dipolar Interaction in Quantum Gases. *Phys. Rev. Lett.* **2002**, *89*, 130401. [[CrossRef](#)] [[PubMed](#)]
62. Roati, G.; Zaccanti, M.; D’Errico, C.; Catani, J.; Modugno, M.; Simoni, A.; Inguscio, M.; Modugno, G. 39K Bose–Einstein condensate with tunable interactions. *Phys. Rev. Lett.* **2007**, *99*, 010403. [[CrossRef](#)] [[PubMed](#)]
63. Tikhonenkov, I.; Malomed, B.A.; Vardi, A. Vortex Solitons in Dipolar Bose–Einstein Condensates. *Phys. Rev. A* **2008**, *78*, 043614. [[CrossRef](#)]
64. Sinha, S.; Santos, L. Cold Dipolar Gases in Quasi-One-Dimensional Geometries. *Phys. Rev. Lett.* **2007**, *99*, 140406. [[CrossRef](#)]
65. Cuevas, J.; Malomed, B.A.; Kevrekidis, P.G.; Frantzeskakis, D.J. Solitons in quasi-one-dimensional Bose–Einstein condensates with competing dipolar and local interactions. *Phys. Rev. A* **2009**, *79*, 053608. [[CrossRef](#)]
66. Huang, C.Q.; Lyu, L.; Huang, H.; Chen, Z.P.; Fu, S.H.; Tan, H.S.; Malomed, B.A.; Li, Y.Y. Dipolar bright solitons and solitary vortices in a radial lattice. *Phys. Rev. A* **2017**, *96*, 053617. [[CrossRef](#)]
67. Ramachandhran, B.; Opanchuk, B.; Liu, X.J.; Pu, H.; Drummond, P.D.; Hu, H. Half-quantum vortex state in a spin–orbit-coupled Bose–Einstein condensate. *Phys. Rev. A* **2021**, *85*, 023606. [[CrossRef](#)]
68. Li, Y.; Liu, J.; Pang, W.; Malomed, B.A. Matter-wave solitons supported by field-induced dipole-dipole repulsion with spatially modulated strength. *Phys. Rev. A* **2013**, *88*, 053630. [[CrossRef](#)]
69. Li, Y.; Liu, Y.; Fan, Z.; Pang, W.; Fu, S.; Malomed, B.A. Two-dimensional dipolar gap solitons in free space with spin–Orbit coupling. *Phys. Rev. A* **2017**, *95*, 063613. [[CrossRef](#)]
70. Huang, C.; Ye, Y.; Liu, S.; He, H.; Pang, W.; Malomed, B.A.; Li, Y. Excited states of two-dimensional solitons supported by spin–orbit coupling and field-induced dipole-dipole repulsion. *Phys. Rev. A* **2018**, *97*, 013636. [[CrossRef](#)]
71. Chiofalo, L.M.; Succi, S.; Tosi, P.M. Ground state of trapped interacting Bose–Einstein condensates by an explicit imaginary-time algorithm. *Phys. Rev. E* **2000**, *62*, 7438. [[CrossRef](#)] [[PubMed](#)]
72. Yang, J.; Lakoba T.I. Accelerated Imaginary-time Evolution Methods for the Computation of Solitary Waves. *Stud. Appl. Math.* **2008**, *120*, 265–292. [[CrossRef](#)]
73. Vakhitov, N.G.; Kolokolov, A.A. Stationary solutions of the wave equation in the medium with nonlinearity saturation. *Radiophys. Quantum Electron.* **1973**, *16*, 783–789. [[CrossRef](#)]
74. Hu, Y.M.; Fei, Y.F.; Chen, X.L.; Zhang, Y.B. Collisional Dynamics of Symmetric Two-Dimensional Quantum Droplets. *Front. Phys.* **2022**, *17*, 61505. [[CrossRef](#)]
75. Luo, Z.H.; Pang, W.; Liu, B.; Li, Y.Y.; Malomed, B.A. A new form of liquid matter: Quantum droplets. *Front. Phys.* **2021**, *16*, 32201. [[CrossRef](#)]

Disclaimer/Publisher’s Note: The statements, opinions and data contained in all publications are solely those of the individual author(s) and contributor(s) and not of MDPI and/or the editor(s). MDPI and/or the editor(s) disclaim responsibility for any injury to people or property resulting from any ideas, methods, instructions or products referred to in the content.